Amorphous WO_3 Films via Chemical Vapor Deposition from Metallorganic Precursors Containing Phosphorus Dopant

E. Brescacin,* M. Basato,* and E. Tondello

Centro di Studio sulla Stabilità e Reattività dei Composti di Coordinazione, C.N.R., Dipartimento di Chimica Inorganica, Metallorganica e Analitica, via Marzolo 1, 35131 Padova, Italy

Received July 31, 1998. Revised Manuscript Received November 12, 1998

Amorphous WO_3 films, doped with phosphorus, have been synthesized by chemical vapor deposition of volatile, low-melting P-substituted tungsten carbonyls. The presence of a small quantity of dopant released by the precursor during its decomposition is sufficient to inhibit the crystallization of the tungsten oxide on the matrix (P/W 2−4 atom % on Si(100) and ca. 10 atom % on KGlass). The nature of the film is scarcely affected by the experimental conditions of deposition (namely p_{O_2} partial pressure) and the quantity of the P dopant is properly tuned by an appropriate choice of the molecular precursor, being in the order $W(CO)_4[P(OEt)_3]_2$ (P/W 1/1) > $W_2(\mu\text{-}PR_2)_2(CO)_8$ (P/W 1/4) > $W(CO)_4(PEt_3)_2$ (P/W 1/10 on KGlass, 1/30 on Si). The films on KGlass exhibit interesting electrochromic properties with a maximum efficiency of 66 cm^2/C.

Introduction

Tungsten oxide is the most important inorganic material for electrochromic applications such as "smart windows" and displays.[1] It is commonly deposited as a thin film on conductive and transparent substrates and then tested for its optical properties by application of a pulsed voltage. A negative pulse induces a blue coloration of the initially transparent material: the process is quite completely reversed by inversion of the potential to positive values.[2] Quantitative parameters of the electrochromic properties of tungsten oxide (efficiency, "colorability", reversibility, and kinetics of the coloration−decoloration process) strongly depend on its structural, morphological, and compositional characteristics and, therefore, on the deposition technique and synthetic conditions. It is known, for example, that in their colored form amorphous layers absorb in the visible spectral range more intensely than polycrystalline ones;[3−7] this fact explains a more pronounced technological interest for the former type.

Normal synthetic procedures that operate at temperatures below 300 °C allow to grow amorphous films without difficulties, but any heating procedures in the presence of oxygen at higher temperatures induces a crystallization of the film. Therefore, amorphous tungsten oxide thin films are deposited mainly on various "cold" substrates either by vacuum evaporation of the pure oxide at 900−1100 °C or by sputtering techniques from metallic or oxidized targets.[2] These methods, however, are of limited industrial interest. Recently different techniques have become available and a chemical vapor deposition (CVD) approach has been applied in this field.[5−7] Starting from $W(CO)_6$ as the precursor, film deposition has been performed in an oxidizing atmosphere. High decomposition temperatures are necessary to obtain pure and stoichiometric layers of tungsten oxide, but under these conditions the films crystallize. Actually satisfactory examples of CVD synthesis at low temperatures cannot be found in the literature; several attempts to grow amorphous films of tungsten oxide under mild conditions starting from the same precursor generally afforded quite poor quality products.[8]

In this work we propose a different approach to the problem: the synthesis of phosphorus-doped tungsten oxide films starting from metallorganic precursors that contain the dopant in the coordination sphere of the metal. It is thus possible to grow amorphous films at higher temperatures, taking advantage of the ability of oxidized phosphorus derivatives to vitrify the host matrix.[9] The single-source approach simplifies the synthetic apparatus and focuses our attention on an interesting chemical problem: the choice of an appropriate precursor. We have synthesized and used some carbonylic derivatives of formula $W_2(\mu\text{-}PR_2)_2(CO)_8$ [R = Me (**2**), Et (**3**)], *trans*- and *cis*-$W(CO)_4(PEt_3)_2$ (**4** and **5**), and *trans*-$W(CO)_4[P(OEt)_3]_2$ (**6**). All these precursors are volatile and stable enough under the operative conditions to be practically useful for CVD processes.

(1) Green, M. *Chem. & Ind.* **1996**, 641.
(2) Granqvist, C. G. *Handbook of inorganic electrochromic materials*; Elsevier: New York, 1995.
(3) Shirmer, O. F.; Wittwer, V.; Baur, G.; Brandt, G. *J. Electrochem. Soc.* **1977**, *124*, 749.
(4) Faughan, B. W.; Crandall, R. S. *Appl. Phys. Lett.* **1977**, *31*, 834.
(5) Davazoglou, D.; Donnadieu, A. *Thin Solid Films* **1987**, *147*, 131.
(6) Davazoglou, D.; Donnadieu, A. *Thin Solid Films* **1988**, *164*, 369.
(7) Maruyama, T.; Arai, S. *J. Electrochem. Soc.* **1994**, *141*, 1021.
(8) Maruyama, T.; Kanagawa, T. *J. Electrochem. Soc.* **1994**, *141*, 2435.
(9) see for ex. Deschanvres, J. L.; Vaca, J. M.; Joubert, J. C. *J. de Phys. VI*, **1995**, *5*, C5−1029.

10.1021/cm980741n CCC: $18.00
Published on Web 01/28/1999

Table 1. Synthetic Conditions of the Films on Si(100).

	N_2 flow (sccm[a])	O_2 flow (sccm[a])	O_2 pressure (mbar)	total pressure (mbar)
A	250	120	1	4
B	120	250	3	4−4.3
C		300	5	5

[a] Standard cubic centimeters per minute.

Moreover, the phosphino derivatives **4**-**6** are cheap and easy to synthesize, and these features increasing their industrial applicability.

The substrate used in the first part of the work was a Si crystal exposing a (100) plane. This material was first considered due to its characteristics of transparency in the MIR region, purity, and atomically flat surface, passivated by a thin layer of inert SiO_2, which make it an ideal substrate for the characterization of deposited films. Furthermore, this material is considered as a possible substrate for devices such as gas sensors, as tungsten oxides can be used for H_2S and NO_x detection.[10,11] In the second part, we will describe the results obtained with CVD deposition on KGlass, a commercial, optically transparent substrate with high electric conductivity. The resulting films were all compared with those obtained from hexacarbonyl tungsten (**1**), with particular attention to the morphology of the deposit and the effect of the dopant on the electrochromic properties.

Experimental Section

The $W_2(\mu\text{-}PR_2)_2(CO)_8$ (**2** and **3**) complexes were synthesized and purified following Hayter's procedure for the dimethylphosphido derivative;[12,13] an increased, almost quantitative yield of complex **3** was obtained by heating the intermediate $(CO)_5W-PEt_2-PEt_2-W(CO)_5$ under vacuum at 210 °C. The $W(CO)_4(PR_3)_2$ (**4**−**6**) derivatives were synthesized as cis/trans mixtures by reaction of $W(CO)_6$ (7 mmol) with a slight excess of PR_3 (17 mmol) in boiling diglyme (25 mL): the cis/trans isomers were isolated and purified by column chromatography (light petroleum ether/5% diethyl ether as eluent; silica gel as stationary phase) and showed physical−chemical properties identical to those reported in the literature.[14] Commercial $W(CO)_6$ was purified by sublimation.

All deposition experiments were performed in a cold-wall reactor using O_2 or N_2/O_2 mixtures as gas carrier. All gases were of >99.999% purity. The precursors were sublimated or evaporated from a small crucible, located close to the reactor, by heating tapes; a thermocouple was used to control the actual temperature. The pressure was measured with a capacitance manometer; the gas flows were controlled by mass flow controllers (2M Instruments).

For the depositions on silicon, the substrate was degreased using boiling trichloroethylene, rinsed with isopropylic alcohol, and then placed on a resistively heated susceptor. The deposition temperature was fixed at 400 °C and controlled with a Pt100 sensor. The overall operative conditions are reported in Table 1.

KGlass is a soda-lime glass covered by a thin layer of polycrystalline SnO_2 (about 150 nm) doped with F; the crystallographic phase is cassiterite. The thickness of the KGlass is 4 mm. This conductive substrate is transparent from 360 to 1800 nm. Its conductivity is equal to 30 Ω/cm^2. The dimensions of the samples were 12 × 18 mm, and the surface covered with the film was confined by a thin foil of aluminum to 1 cm^2. The substrate was degreased by washing with water and soap, rinsed with doubly distillated water and isopropyl alcohol, and finally located on the resistively heated susceptor. The temperature of the heating element was controlled by a thermocouple positioned on the surface of the substrate shielded by the aluminum. The samples were deposited at 300, 350, and 400 °C. Average film thickness was 65 nm, the greatest difference being less than 20 nm. The operative condition used for these deposits is reported in line A of Table 1.

Each film is labeled with the number of the complex precursor followed by a capital letter indicating the condition of deposition.

X-ray photoelectron spectroscopy (XPS) analyses were performed with a Perkin-Elmer Φ 5600ci spectrometer with monochromatized Al Kα radiation (1486.6 eV). The working pressure was less than 1.8×10^{-9} mbar. The spectrometer was calibrated by assuming the binding energy (BE) of the $Au4f_{7/2}$ line at 83.9 eV with respect to the Fermi level. As an internal reference for the peak positions the C1s peak of hydrocarbon contamination was assumed to be 284.8 eV. The standard deviation in the BE values of the XPS lines was 0.10 eV. After a Shirley-type background subtraction, the raw spectra were fitted using a nonlinear least-squares fitting program adopting Gaussian−Lorentzian peak shapes for all the peaks. The atomic compositions were evaluated using sensitivity factors as provided by Φ V5.4A software. Depth profiles were carried out by Ar^+ ions sputtering at 0.5−1.5 keV, 0.4 mA cm^{-2} beam current density with an argon partial pressure of 5×10^{-8} mbar.

IR measurements were performed on a FTIR Bruker IFS 66 instruments. Samples on silicon were analyzed in transmittance mode, whereas the reflectance mode with an incident angle of the radiation at 70° out-of-normal was applied for the KGlass samples. XRD data were recorded on a Philips diffractometer with thin film equipment, employing Cu Kα radiation (λ = 1.54 Å), incident at 1° with respect to the surface.

Atomic force microscopy (AFM) images were collected by a Park Scientific Autoprobe CP microscope in contact mode, in air and at room temperature. The cantilever was a Park Scientific Instruments Microlevel 0.6 μm. The only image adjustment was connected to the correction for the drift of the tip ("flattening").

Electrochromic measurements were performed in a UV cell (20 × 20 mm) containing $LiClO_4$ (0.3 M)/PC (anhydrous propilen carbonate) as electrolytic solution. KGlass was used as counter electrode and, covered with the tungsten oxide film, as working electrode. The reference was an $Ag/AgClO_4$ ($LiClO_4$ O.3 M)/PC electrode (0.29 V with respect to NHE). The contacts to electric cable were obtained by a silver glue and protected with epoxidic resin. Pulsed voltages were applied by a potentiometer/coulombometer EG&G Model 273 (P.A.R. Instruments) and the spectrophotometric data were collected by a UV−vis−NIR Varian Cary 5E.

Results and Discussion

Depositions on Si(100). *Film Deposition from $W(CO)_6$ [Samples 1A, 1C].* As previously stated, hexacarbonyl tungsten is our reference. The oxidation of this complex on a Si(100) substrate gives a tungsten oxide film, with a probable oxygen deficiency. Some XPS data of the samples are collated in Table 2.

The carbon content of $W(CO)_6$ (**1**) (not reported), on the surface and in depth, is below 1%, and quantitative analysis shows that the stoichiometry of the film on the surface is near to the ideal one (W/O = 1/3) within the experimental error. The position of the tungsten $W4f_{7/2}$ photoelectronic peak (35.67 eV) is in agreement with a highly oxidized species and with the corresponding peak

(10) Antonik, M. D.; Schneider, J. E.; Wittman, E. L.; Snow, K.; Vetelino, S. F.; Lad, R. J. *Thin Solid Films* **1995**, *256*, 247.
(11) Xu, Z.; Vetelino, J. F.; Lec R.; Parker, D. C. *J. Vac. Sci. Technol. A* **1990**, *8*, 3634.
(12) Hayter, R. G. *Inorg. Chem.* **1964**, *3*, 711.
(13) Basato, M. *J. Chem. Soc., Dalton Trans.* **1985**, 91.
(14) Poilblanc, R.; Bigorgne, M *Bull. Soc. Chim. Fr.* **1962**, 1301.

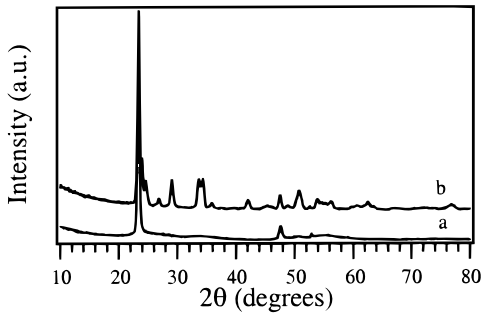

Figure 1. XRD spectrum of the sample 1A before (a) and after (b) thermal treatment at 400 °C for 48 h.

Table 2. Surface XPS Data

	W4f$_{7/2}$, eV (fhwm)	O1s, eV (fhwm)	P2p$_{3/2}$, eV (fhwm)	W/P on surface
WO_3 powder	35.61 (1.25)	530.53 (1.66)		
1A	35.67 (1.57)	530.69 (1.44)		
2A	35.78 (1.48)	530.80 (1.52)	133.06 (1.60)	80/20
2C	35.57 (1.37)	531.02 (1.57)	133.31 (1.65)	83/17
3A	35.92 (1.31)	530.99 (1.52)	133.18 (1.49)	78/22
3C	35.77 (1.48)	531.07 (1.76)	132.92 (1.46)	74/26
4A	35.57 (1.29)	530.67 (1.33)	133.15 (1.76)	98/2
4B	35.98 (1.37)	531.08 (1.46)	133.40 (1.50)	97/3
4C	35.76 (1.32)	530.83 (1.43)	133.28 (1.50)	96/4
5B	35.59 (1.28)	530.71 (1.38)	132.90 (1.55)	96/4
6A	36.16 (1.59)	531.51 (1.93)	133.87 (1.65)	54/46

measured for tungsten oxide powders (35.61 eV). The O 1s peak (530.69 eV) appears in accordance with both the measured (530.53 eV) and the literature data for tungsten oxide.[15]

Under the above-mentioned conditions (A−C of Table 1) with the substrate at 400 °C, the layers obtained were polycrystalline in all cases. With slowly grown films (conditions A of Table 1 and the temperature of the precursor just below 60 °C), the XRD pattern is constituted of a single peak at 23.4° (second order at 47.6°), indicating a strong preferential orientation along the [001] axis (see Figure 1a). The preferential orientation of crystallites can be partially or even completely removed either by growing the deposit under drastic conditions (high partial pressure of oxygen, high flow of the precursor) or by prolonged annealing at high temperatures in air. In particular, after annealing, we have observed the appearance of additional signals at 24.0° and 24.7° that, along with the signal at 23.4°, can be ascribed to a triclinic phase (Figure 1b).[16] Supposing that no phase transition occurs during this thermal treatment, it can be stated that also the as-deposited material has a triclinic crystallographic structure.

Preferentially oriented films show an infrared spectrum (see Figure 2 A) quite different from powder samples. In the range between 500 and 1000 cm^{-1}, the absorption band of the tungsten oxide matrix is broad and the peak at 810 cm^{-1} appears now as a shoulder. It is important to notice the presence of a new additional peak at about 567 cm^{-1}, not found in unoriented samples.

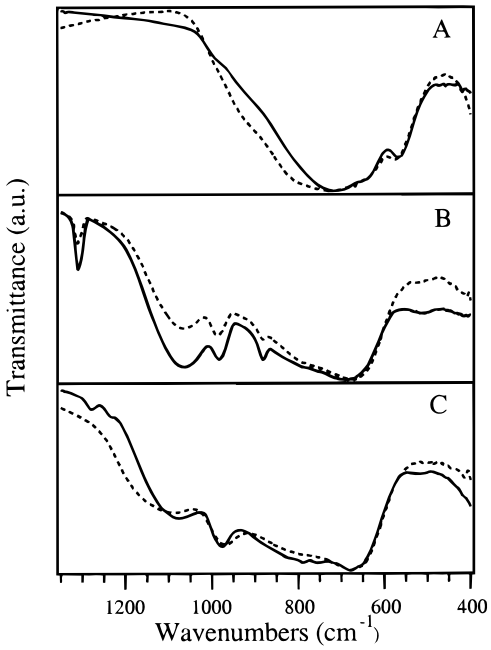

Figure 2. (A) FT-IR spectra of the samples 1A (plane line) and 1C (dotted line) (sample 1C present a more "rough" XRD pattern with respect to the sample 1A; similarly, the infrared signal is quite more enlarged); (B) FT-IR spectra of the samples 2A (plane line) and 2C (dotted line); (C) FT-IR spectra of the samples 3A (plane line) and 3C (dotted line).

Film Deposition from $W_2(\mu\text{-}PR_2)_2(CO)_8$ with R = Me, Et [Samples 2A, 2C and 3A, 3C]. These complexes are binuclear red compounds sublimating at about 60 °C. The phosphorus is bridged between two tungsten atoms and therefore it is easy to preview that these compounds will release a good quantity of dopant in the resulting deposits. The presence of an ethyl group in complex **3** increases the electronic charge on the phosphorus atoms and their ease of oxidation and correspondingly reduces the possibility of its escaping from the matrix; this is confirmed by the slightly higher content of dopant on the surface with respect to the samples 2 (from 22 to 26% with respect to W + P). Mass spectrometry analyses of homologous bis(dimethylphosphido)molybdenum and mixed molybdenum−tungsten compounds reveal the presence of trimethylphosphine in their fragmentation pattern;[17] it is reasonable that this is the way most phosphorus escapes from the film after the thermal decomposition of these complexes. On the other hand, the same analytical tool shows that the W(μ-P)$_2$W ring is certainly very stable; this aspect allows us to preview an intrinsic homogeneity, even at an atomic level, of dopant distribution in the resulting film.

XPS data concerning the films on silicon substrates are reported in Table 2. The metal-to-dopant ratio W/P on the surface for a specific sample does not markedly depend on growth conditions. It is clear that the different oxygen partial pressures applied in our experiments (1−5 mbar) do not play an important role in the decomposition pattern of the complex. The resulting concentration of dopant and of oxygen is lower in the bulk than on the surface (medium ratio W/P 87/13), but this is certainly due to a marked phenomenon of

(15) Moulden, J. F.; Stickle, W. F.; Sobol, P. E.; Bomben, K. D. *Handbook of X-ray Photoelectron Spectroscopy*; Perkin-Elmer Corp.: Minnesota, 1992.

(16) Joint Committee for Powder Diffraction Standards, JCPDS card no. 321395 (Joint Committee for Powder Diffraction Standards, Swarthmore, Pennsylvania, 1992.

(17) Johnson, B. F. G.; Lewis, J.; Wilson, J. M. *J. Chem. Soc. (A)* **1967**, 1446.

preferential sputtering during the analysis. Despite this, the XPS depth profiles reveal a constant distribution of the phosphorus in the bulk and confirm the initial hypotheses.

The XPS tungsten signal is positioned at slightly higher binding energies values than previously reported ($\Delta_{aver} = 0.1$ eV). Moreover, a shoulder is often found in the range 34.2−34.6 eV, easily associated with the lower oxidation states of the metal.[18] All the gathered information is in accordance with the effects of the presence of phosphorus in the matrix; an increased ionicity and an actual distortion of the crystallographic environment generate tungsten sites with lower coordination and therefore lower effective oxidation state. The BE of the superficial phosphorus is coherent with high oxidation state species (132.9−133.3 eV).

The presence of the dopant in the lattice effectively alters the tridimensional structure, and the samples show an XRD pattern without any characteristic diffraction peak. The samples are completely amorphous and no variation was observed, even after a prolonged thermal treatment in air (24 h at 450 °C).

Infrared absorption of the phosphate groups in the FT-IR spectra dominates the pattern (see Figure 2B,C) and demonstrates that the local structure is reasonably different for films 2 and 3. In fact, the signals in the higher frequency region (900−1400 cm^{-1}) are quite well defined in the samples 2; the P−O stretching signals are positioned at 1062 and 986 cm^{-1} and a typical P═O absorption is found at 1310 cm^{-1}. At lower wavenumbers, absorptions due to P−O−P systems (880 and about 690 cm^{-1}) are superimposed on the signals connected with the "W−O" lattice vibration modes. The signal in this region is not structured and this is compatible with an amorphous sample. On the other hand, undefined and broad absorptions and the absence of signals relative to "P═O" species characterize this IR region in samples 3; this feature is reproducible and can be associated with the different nature of the phosphate species in the matrix.

Film Deposition from trans- ***(4)*** *and cis-$W(CO)_4(PEt_3)_2$* ***(5)***. The chemical nature and reactivity of these complexes are closer to those of the hexacarbonyl derivative rather than of complexes **2** and **3**.

Compound **4** melts at 54 °C and the cis isomer at 74 °C. In our experiments we heated the precursors at a temperature higher (about 10 °C) than its melting point. The possibility of handling a precursor in the liquid phase is interesting in a CVD process, because it allows a better control of its flow to the substrate, taking advantage of its tuneable vapor pressure (that is strongly temperature-dependent) and of the homogeneity of the evaporating surface (that guarantees a constant evaporation flow).

The phosphorus is present as phosphine directly linked to the metal. This type of ligand can be easily lost in a typical process of thermal decomposition and therefore, due to its high volatility, it is reasonable that a low content of dopant will characterize the resulting oxide films. On the other hand, the possibility of oxidizing the ligand on the substrate is related to its time of permanence on the heated surface, and from this point of view, it is reasonable to suppose that different growth conditions can significantly modify the resulting deposit and modulate the doping.

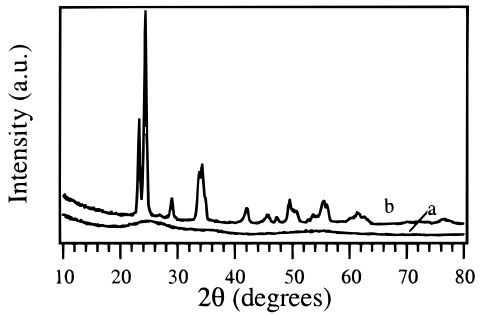

Figure 3. XRD spectrum of the sample 4A before (a) and after (b) thermal treatment at 400 °C for 12 h.

The experimental results confirm the first hypothesis. The superficial phosphorus content is very low under all synthetic conditions for both the precursors (the complex **5** was studied in film deposition only for the B conditions of Table 1). It can be quantified in the range between 2 and 4% with respect to the metal (a real doping, considering that the matrix is tungsten oxide of formula WO_3). This quantity is only indicative of a reduced presence of the dopant; in fact, because of the low sensitivity to phosphorus due to the small cross section of this element combined with the low atomic percentage, the XPS quantitative measurements should be compared one to another rather than taken as absolute figures. In other words, these phosphorus contents cannot be considered significantly different, and the trend observed on films 4A, 4B, and 4C (higher oxygen partial pressure, more dopant on the surface), if real, demonstrates the small effect of the growing conditions on the nature of the resulting deposits. The phosphorus content in film 5B is also not significantly higher than that determinated on the corresponding film from complex **4**. The preferential sputtering phenomenon did not allow us to collect reliable information about the distribution of the dopant in the bulk of the film.

From a qualitative point of view, the XPS analysis (Table 2) shows films with characteristics similar to those obtained from $W(CO)_6$. The tungsten signal does not present any component due to oxidation states lower than VI, and the phosphorus is completely oxidized.

All the layers deposited under these conditions appear to be amorphous. This aspect is really interesting because it demonstrates that small quantities of phosphorus (a real doping in this case) are able to inhibit the crystallization of the growing matrix of tungsten oxide. However, a postdeposition thermal treatment at 400 °C is sufficient to convert this matrix to a crystallized form (Figure 3). A detailed analysis of the XRD spectrum allowed us to identify the crystallographic phase as orthorhombic.[19] This fact demonstrates that the phosphorus content is too low to maintain the "destructuration" of the matrix after a thermal treatment. It is also interesting to observe that the phosphorus is able to drive the crystallization of the film to

(18) Yao, J. N.; Chen, P.; Fujishima, A. *J. Electroanal. Chem.* **1996**, *406*, 223.

(19) Joint Committee for Powder Diffraction Standards, JCPDS card no. 201324 (Joint Committee for Powder Diffraction Standards, Swarthmore, Pennsylvania, 1992.

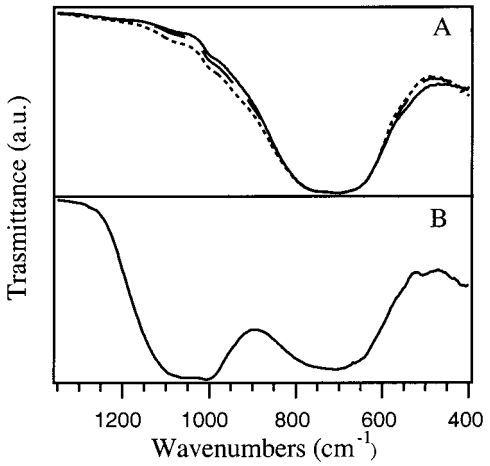

Figure 4. (A) FT-IR spectra of the samples 4A (plane line), 4B (semidotted line) and 4C (dotted line); (B) FT-IR spectra of the sample 6A. FT-IR spectrum of sample 5B, not shown, does not significantly differ from the spectrum obtained for sample 4C (noticeably, samples 4C and 5B present the same phosphorus content).

a crystallographic form different (orthorhombic) from that using the hexacarbonyl derivative as precursor (triclinic).

FT-IR spectra of the films obtained from compounds **4** and **5** show a broad, unstructured signal in the region between 600 and 1000 cm^{-1} (Figure 4 A); this feature is perfectly compatible with the amorphous state of the samples. The contribution of the phosphate species to the absorption peak is very reduced and appears on the higher energy side of the peak (at about 1000 and 1075 cm^{-1}) as P−O stretching. By normalizing the FT-IR signals of layers obtained under different conditions (from A to C of Table 1) and considering absorption peak intensities as directly related to the phosphorus content in the matrix (the measurements was in transmittance mode), it is possible to recognize, and therefore confirm, the same trends previously described for the XPS surface analysis. The FT-IR analysis also confirms quantitatively the reduced content of dopant and the small effect of the oxygen partial pressure on the doping of both the films 4 and 5.

From these considerations stems the possibility of using a mixture of the two isomers as a precursor. This approach simplifies the overall procedure. In fact, the complexes are both present in the reaction mixture after their synthesis from $W(CO)_6$ and PEt_3, and no separation procedure needs to be performed. Second, the mixture has a lower melting point and is easier to vaporize, which is always favorable in a CVD process.

*Film Deposition from trans-$W(CO)_4$ $[P(OEt)_3]_2$ (**6**).* The phosphite complex is certainly another interesting precursor for thin film deposition. It is easily synthesized and handled in air without problems. It melts at 56 °C and therefore it can be used in deposition experiments from its liquid phase.

The analysis of the composition on the surface was performed by XPS measurements, as usual. The result was interesting, as the metal-to-dopant ratio on the surface was quite close to 1. This datum is surprising because it indicates that the deposition behavior of this precursor is markedly different from that of **4** and **5**, despite the chemical and physicochemical analogies

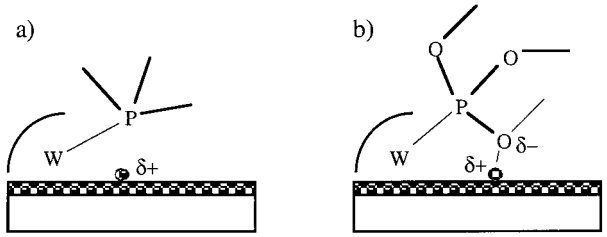

Figure 5. A possible scheme for the different behavior of compounds **4** and **5** (a) with respect to the complex **6** (b). $\delta-$ and $\delta+$ indicate partial charge densities on the oxygen and, e.g., on W^{n+} sites, respectively.

between these complexes. In fact, these bis-substituted complexes present similar volatility and certainly the W−P bond in the bis-phosphite compound **6** is weaker than in **4** and **5**. At the same time, the triethyl phosphite and triethylphosphine ligands have the very close boiling points of 160 and 156 °C, respectively. Being highly improbable that this complex would follow a different decomposition pathway with respect to the complexes **4** and **5**, the deposition mechanism most likely involves in this case an interaction between $P(OEt)_3$ and the growing oxide matrix, which increases the contact time of the phosphite on the heated substrate and correspondingly increases its probability of decomposition on the surface. This interaction, which appears limited with triethylphosphines, reasonably involves the ethoxy oxygen and the Lewis acid sites like W^{n+} on the surface (see Figure 5).

The depth profile of the films, despite the preferential sputtering that alters the real atomic ratios (experimental medium W/P ratio in the matrix, 83/17), confirm the presence of conspicuous quantities of dopant in the bulk. In this case we are dealing with a genuine phosphotungstic glass. No carbon contamination in the matrix was identified; the oxidizing conditions were strong enough to convert all the carbon species in volatile CO and CO_2.

Qualitatively speaking, the XPS characteristics of species on the surface are similar to what seen for precursors **2** and **3**. The main $W4f_{7/2}$ photoelectronic peak is sensibly shifted to higher binding energies (36.16 eV), in agreement with the increased polarity of the matrix; the metal is more charged in a matrix where the phosphorus moves onto itself the electronic charge of the surrounding oxygen atoms. Furthermore, a well-defined shoulder is present at 34.7 eV due to tungsten species in lower oxidation states. It is reasonable to suppose that, even in this case, the oxygen geometry imposed by the dopant induces some highly distorted sites of tungsten in which the metal has an effective reduced coordination and, correspondingly, charge. The phosphorus is present, as expected, in high oxidation state.

It is evident that under these conditions the films are thoroughly amorphous and no thermal treatment at 450 °C could achieve the crystallization of the matrix.

FT-IR spectra of the film are quite different from those previously shown for **2** and **3** complexes (Figure 4B). The absorptions relative to the "W−O" and "P−O" systems are clearly separated. The former (centered at about 700 cm^{-1}) is broad and undefined, as typical for amorphous systems; the latter (1050 cm^{-1}) is intense and easily associated to P−O stretching of simple PO_3

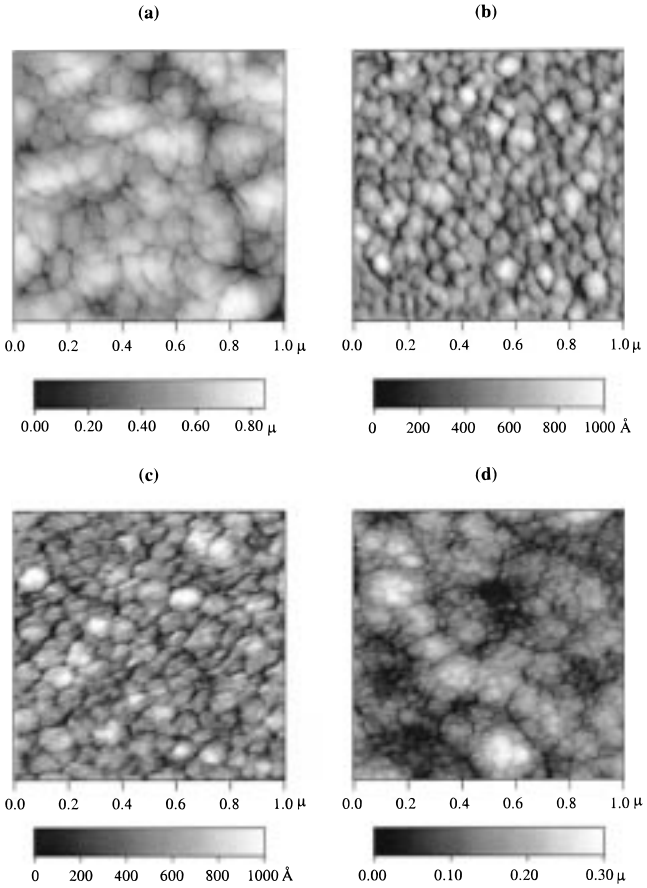

Figure 6. AFM images of samples grown on silicon substrate: (a) sample 1C, (b) sample 2C, (c) sample 3C, (d) sample 4C.

Table 3. Morphological Data of the Samples Deposited at Higher Oxygen Partial Pressure and Shown in Figure 6

	medium height (Å)	surface area (μ^2)	roughness (Å)
1C	6861	19.43	1326
2C	697	2.70	176
3C	791	4.91	202
4C	1849	6.65	565

or PO_4 units. These data suggest the possibility that the "PO_3" units in $P(OEt)_3$ are conserved during the event of decomposition, generating a highly connected structure, branched and finely mixed with "WO_n" units.

Film Morphology by AFM Analysis. Morphological information is very important from an electrochromic point of view. Silicon wafers are atomically flat, and the surface presents nearly the same reactivity toward all of the complexes used in this work. This suggests to us that the morphology of the film strongly depends on the decomposition process of the precursor on the surface and, correspondingly, on the dopant content in the film.

As shown in Figure 6a, polycrystalline iso-oriented tungsten oxide films obtained from hexacarbonyl tungsten appear very rough and with an extended surface area. Introduction of little amounts of phosphorus in the film (samples 4) produces a drastic attenuation of these characteristics, quantified in the Table 3. The *x,y* dimensions of the particles are certainly reduced (estimated below 50 nm) and they appear collected in macrostructures similar to clusters.

Choosing a different kind of precursor, which significantly increases the dopant content in the matrix, the surface appears more even and the roughness is decreased. The precursors **2** and **3** generate films with similar morphological characteristics, where the particles present lateral dimension in the range between 50 and 100 nm and the texture resembles a patchwork-like picture.

Table 4. XPS Surface Analysis on the Samples Grown on KGlass

	$W4f_{7/2}$, eV (fhwm)	O1s, eV (fhwm)	$P2p_{3/2}$, eV (fhwm)	W/P on surface
1A (300 °C)	35.78 (1.32)	530.76 (1.34)		
1A (400 °C)	35.52 (1.20)	530.43 (1.36)		
3A (300 °C)	35.99 (1.29)	531.12 (1.58)	133.50 (1.68)	81/19
3A (400 °C)	36.05 (1.33)	531.17 (1.57)	133.64 (1.48)	76/24
4A (300 °C)	35.87 (1.33)	530.95 (1.45)	133.38 (1.82)	91/9
4A (400 °C)	35.62 (1.37)	530.73 (1.50)	133.13 (1.80)	81/19
6A (300 °C)	36.17 (1.98)	531.44 (1.93)	133.90 (1.72)	51/49

Generally speaking, the images show the evolution of a polycrystalline material to the typical morphology of a vitreous, glass-like matrix. The process is substantially a phenomenon of flattening (easily identified considering the *z*-scale in the figures) with disgregation of the crystallites.

Thermal treatment did not affect the morphology of the samples rich in dopant and, quantitatively, no relevant differences were identified in the roughness and surface area data; on the contrary, the samples grown from precursors **4** and **5** were seriously damaged in the crystallization process.

Depositions on KGlass. In this part of the work we have considered three different precursors (**3**, **4**, and **6**) for the deposition of P-doped tungsten oxide films on KGlass. In the previous section we have verified that all of these complexes release a different quantity of dopant on the silicon matrix under the same conditions. In Table 4 we list the situation discovered by XPS analysis on KGlass at different deposition temperatures.

Complex **3** releases on the surface 19 atom % of dopant with respect to W + P at 300 °C and is only a little more efficient at higher temperatures (24 atom % at 400 °C); these data do not differ considerably from the results obtained on the Si(100) substrates discussed previously. It is reasonable to conclude that this complex is relatively insensitive both to the temperature and the nature itself of the substrate; in fact, it appears that, above the decomposition temperature, the evolution of the complex on the surface is relatively independent of these parameters. The opposite behavior was observed for complex **4**; it released 9 atom % of phosphorus at 300 °C, 14 atom % at 350 °C (not reported in the table), and 19 atom % at 400 °C (with respect to W + P). These data confirm the influence of the temperature on the decomposition efficiency of the phosphine complex and, remembering that the dopant is present in trace amount in the corresponding films grown on silicon at 400 °C, it appears evident that the nature of the substrate plays an important role in this case. This fact can be ascribed to the ability of the polycrystalline SnO_2 layer to capture and oxidize the triethylphosphine liberated in the decomposition of the complex. The precursor **6** was decomposed only at 300 °C, but even at this temperature, the percentage of dopant in the film obtained was 50 atom % with respect to W + P. We observed an analogous behavior on silicon substrate and it was rationalized with the presence of the ethoxy oxygens

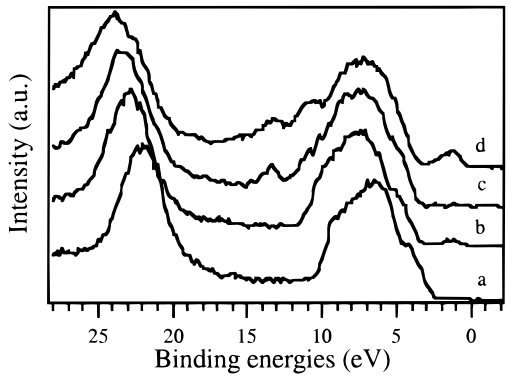

Figure 7. Valence band of the samples 1A at 400 °C (a), 1A (b), 3A (c), and 6A (d) at 300 °C.

that link the phosphito derivative to the acids sites on the growing surface favoring a long contact time and the oxidation reaction on the heated surface. In this case, the reactivity of this surface can justify an analogous result at lower temperatures.

From a qualitative point of view, XPS analysis demonstrates the presence of species in high oxidation state on the surface of the samples. By comparison with analogous films obtained at 300 and 400 °C starting from $W(CO)_6$, the BE of $W4f_{7/2}$ appears to be slightly shifted toward higher values in the samples obtained from complex **4** and clearly positioned at 36.0−36.2 eV for samples 3 and 6. The trend is clear: the more dopant that is present in the film (and, therefore, the more "ionic" the lattice, considering that the binding energy of phosphorus in all the samples is compatible with the presence of phosphates), the higher the BE of the metal. An analogous trend is observed for oxygen.

In addition, XPS depth profile analysis of these samples confirms the homogeneous distribution of the dopant in the matrix, even if the absolute value of this doping and information about the oxidation state of the species cannot be extracted from these measurements due to the problems connected to preferential sputtering of oxygen and phosphorus during the analysis.

As an interesting tool of comparison, the valence band of these systems can be considered. In Figure 7 the spectra of samples 1, 3, and 6 deposited at 300 °C, and of 1 obtained at 400 °C (and therefore polycrystalline) are represented. Some characteristics are evident: the O2s and O2p signals related to system 1 are more "structured"; the presence of phosphorus in the matrix causes the broadening of the oxygen photoemission peaks that can be temptatively correlated to the presence of oxygen in different chemical states or, in other words, to the amorphous condition of this layer. The oxygen atoms linked to the dopant, present in high percentage on the surface, are reasonably responsible for the presence of two supplementary peaks in the valence band spectra at 13.4 and 10.5 eV in samples 3 and 6. Moreover, it is sometimes possible to observe the presence of a little photoelectronic peak at higher kinetic energies (BE about 1.4 eV) due to W(V) species in the matrix;[20,21] in this case, it appears particularly evident for sample 6, but it is present even in sample 1 (see Figure 7b,d). It is reasonable that the synthetic procedure or conditions cannot complete the oxidation of the matrix in the presence of a phosphine ligand (PR_3 or, particularly, $P(OEt)_3$), but it is also possible that tungsten in these cases is captured in sites at low coordination and its effective oxidation state is lowered. The presence of reduced metal oxide in the films is evidenced by a residual blue coloration (that will be later quantified by UV measurements) and with the presence of greater fhwm values or little low-BE components on the XPS principal signals.

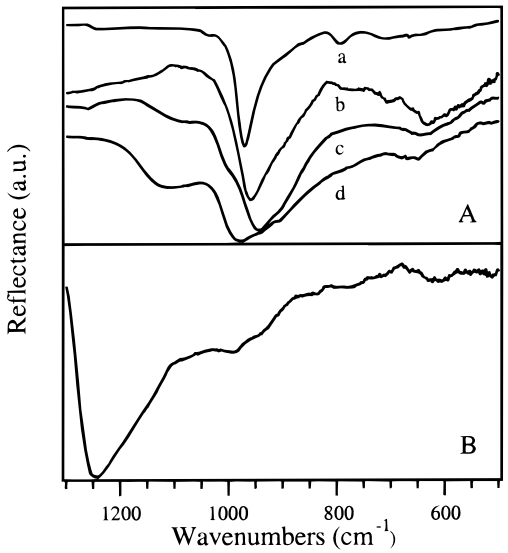

Figure 8. (A) FT-IR reflectance spectra of samples 1 grown at 400 °C (a), 1 at 300 °C (b), 4 (c), and 3 (d) at 300 °C on Kglass; (B) FT-IR reflectance spectrum of the samples 6 on Kglass.

XRD data confirm the above-discussed results; all the samples are amorphous with exception of the film 1 grown at 400 °C and partially of the layer 4 at 300 °C. Moreover, from these data it is possible to verify that the crystallographic phase of sample 4 is different from what observed on 1. The presence of a peak at 23.4° with a shoulder at 24.1° (second order at 47.9°) is compatible with an orthorhombic phase of the film (plans 001 and 020, respectively), in agreement with the analogous films on Si(100). The corresponding XRD spectrum of sample 1 (signal at 23.35° and second order at 47.7°) indicates that it maintains the same triclinic phase observed over silicon. Anyway, it is important to observe that on this substrate the amorphous condition can be reached only with dopant percents over 10 atom %, and this demonstrates that a polycrystalline substrate can facilitate the crystallization of the tungsten oxide matrix.

Infrared spectra of samples 1−6 collected in reflectance mode appear interesting (Figure 8). The reduced absorptions centered around 600−800 cm^{-1} and the presence of intense signals over 850 cm^{-1} can be justified with the appearance of the Berreman effect.[22,23] In fact, the strong absorptions observed, in addition or substitution of the common transversal modes, are

(20) Fleish, T. H.; Mains, G. J. *J. Chem. Phys.* **1982**, *76*, 780.

(21) Colton, R. J.; Guzman, A. M.; Rabalais, J. W.*J. Appl. Phys.* **1978**, *49*, 409.

(22) Göttsche, J.; Hinsch, A.; Wittwer, V. *Proc. Soc. Photo-Opt. Instrum. Engr.* **1992**, *1728*, 13.

(23) Harbecke, B.; Hainz, B.; Grosse, P. *Appl. Phys. A* **1985**, *38*, 263.

connected to the longitudinal vibrational mode of the surface species (in this case, W−O stretching), which normally requires a *p*-polarized infrared probe. In our case, the high infrared reflectant power of the SnO_2 conductive film and the many reflections of the infrared ray in the measurement apparatus can justify a possible strong polarization of the probe and therefore the appearance of this effect. Moreover, a theoretical analysis of the phenomenon reveals that the film thickness is important for the definition of the intensity ratio between longitudinal and transversal absorptions: in this case, the deposits are in a range of thicknesses that favors the former ones, and at the typical region for W−O transversal stretching frequencies, the absorptions appear strongly reduced. Important information can be obtained by comparison with the spectra of the film 1 grown at 300 and 400 °C (see Figure 8 A, curves a, b); in fact, polycrystalline films show a sharp (narrow) and intense signal (at 970 cm^{-1} in this case), while a reduced crystallinity and density (or even a complete amorphous state) determines the broadening of the absorption and a progressive shift toward lower wavenumbers (960 cm^{-1} for the sample 1 grown at 300 °C). On the basis of this observation, it is clear that the experimental spectra of samples 3 and 4 (Figure 8 A, curves c, d) present the characteristics of the unstructured layers with a signal at about 950 cm^{-1}. In addition, two absorptions relative to the phosphate groups are clearly present at about 990 (shoulder) and 1100 cm^{-1}, with intensity proportional to the different phosphorus content previously quantified by XPS analysis. The signals on the lower wavenumber side of the spectrum are too low and undefined to obtain significative information.

Particularly different is the infrared absorption of the glassy matrix of film 6 (Figure 8B). The main signal appears at 1245 cm^{-1}, in a typical region for P═O stretchings. However, the high intensity of the absorption with respect to the other systems suggests the possibility that this signal is due to the Berreman effect too. In fact, in this case, the nature of the sample is clearly glassy and its dielectric behavior (or, in other words, the response of the matrix in the presence of an electromagnetic field as an infrared probe) is certainly different from that of the previous samples. It is reasonable that this absorption is connected to LO stretching mode of "P−O" systems while the TO stretching mode of P−O and W−O systems are present as reduced shoulders at 989 and 944 cm^{-1}.

AFM analysis does not reveal any important information: the films are too thin and the morphology is heavily dominated by the substrate.

Electrochromic Behavior. The electrochromic behavior of the films was tested for the lithium insertion. Pure tungsten oxide films obtained starting from $W(CO)_6$ represented our reference on the efficiency of the phosphorated systems grown under similar synthetic conditions. These as-grown samples present a small oxygen deficiency that generates an initial blue coloration, as quantified by UV−NIR measurements (Figure 9 A), due to a broad absorption peak in the NIR region. However, after negative polarization of the material, the coloration strongly increases and a difference of up to 0.54 in absorbance units can be obtained at 700 nm at

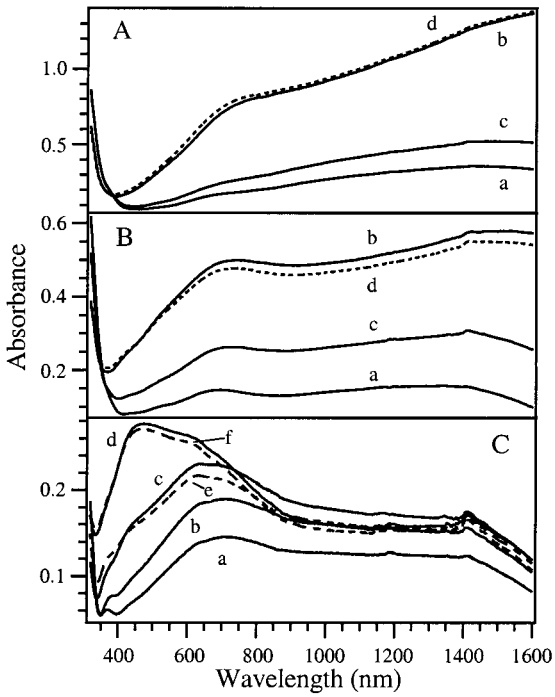

Figure 9. (A) UV spectra of the samples 1: (a) as grown, (b) after polarization at −1 V with respect to $LiClO_4/AgClO_4/Ag$, (c) after repolarization at 0.5 V (d) after new repolarization at −1 V. (B) UV spectra of the samples 4: (a) as grown, (b) after polarization at −1 V with respect to $LiClO_4/AgClO_4/Ag$, (c) after repolarization at 0.5 V, (d) after new repolarization at −1 V. (C) UV spectra of the samples 6: (a) as grown, (b) after polarization at −0.3 V with respect to $LiClO_4/AgClO_4/Ag$, (c) after polarization at −0.5 V, (d) after polarization at −1 V, (e) after repolarization at 0.5 V (dotted line), (f) after new repolarization at −1 V (dotted line).

−1 V (with respect to our reference electrode). The sample maintained some blue coloration even after positive polarization at 0.5 V. All phases of the process are quite slow: 2−3 s in the coloration and 50−60 s to reach a stationary condition under positive potentials. Coloration efficiency was measured at 650 nm and was quantified as 43 cm^2/C; this value is comparable with the data present in the literature for films obtained by different techniques.[6,24]

The as-deposited samples 3 present a reduced initial coloration as the synthetic procedure generates films with a low degree of insaturation. However, the coloration process (the potential applied was −1 V, as for the previous films) appears limited with respect to the reference; under these conditions, in fact, the absolute value of absorbance at about 700 nm was 0.4 (corresponding to an absorbance increase of about 0.37). Moreover, the absorption in the NIR region appears to be much lower than in samples 1. Also the decoloration process appears difficult and the absorbance cannot reduced below 0.15 (700 nm) even after application of a 0.5 V potential for 1 min. The subsequent recoloration process at −1 V reproduces the initial result.

Electrochromic efficiency data on these samples are, on the contrary, particularly interesting. The absolute value obtained at 650 nm was 66 cm^2/C for all the samples. In other words, the tungsten species present

(24) Donnadieu, A.; Davazoglou, D.; Abdellaoui, A. *Thin Solid Films* **1988**, *164*, 333.

in the matrix are particularly active in the coloration process even if, on the basis of the colorability data and considering the corresponding charge injection, they cannot be easily reduced and the reduction process is limited to a low number of tungsten sites in the matrix.

An intermediate situation characterizes the samples obtained from the precursor 4 (Figure 9B). The as-deposited layers, independent of the growing temperature, are slightly colored as for samples 1 (see the reduced absorption in the UV−NIR spectra), but the colorability, i.e., the absorbance obtained in determinate conditions, shows a similar behavior to the samples 3: 0.5 at 700 nm with polarization at −1 V, corresponding to an absorbance variation of about 0.35; an incomplete decoloration process even for prolonged application of 0.5 V potential; quite efficient recoloration process at −1 V; and, finally, as in samples 3, the NIR region absorption intensity appears to be depressed with respect to the visible absorption. The electrochromic efficiency of these samples is 44 cm^2/C and it raises to about 50 cm^2/C for 120 nm thick samples.

Both these phosphorated precursors generate films with particularly stable coloration in air: the blue coloration can be easily preserved for some days if the samples are kept in a desiccator.

Precursor 6 generated vitreous films with a high phosphorus content. The as-deposited layers are blue and the UV spectra resemble those of the previous samples, with the exception of the absorption in the NIR region that appears clearly lowered (Figure 9C, curve a). The coloration process is in this case particularly interesting. The application of a small negative potential to this film (−0.3 V) produces further coloration of the material (coloration efficiency was calculated as 19 cm^2/C), and after polarization at −0.5 V, a small increase in absorbance is observed at all frequencies (Figure 9C, curves b, c). In this situation, however, a new band begins to appear at about 460 nm which, by application of more negative potentials (until −1 V), increases and becomes predominant, even if the maximum is limited to 0.28 in absorbance (curve d). Correspondingly, the coloration of the sample becomes brown and the absorptions at wavelengths over 750 nm are depressed. The material in this case appears modified; W(V) sites, which are responsible for the absorptions at 650 nm and in the NIR region of the spectra and which are generated in the deposition process and by initial polarization processes at low potentials, are partially altered at more negative potentials. The application of a positive potential (0.5 V) and the subsequent repolarization at −1 V (Figure 9C, curves e, f) reveal that the new reversible system absorbs at 465 nm; at the same time, the absorptions at higher wavelengths seem to be unaltered as if the W(V) species were "deactivated".

XPS analysis on these samples before and after the coloration process is frequently used in the literature to confirm and clarify the evolution of the system. As previously stated, the W4f double peak of samples 1, 3, and 4 appeared before the coloration process to be well-defined or, for samples with a minimal blue coloration, slightly broadened and tailed on the low-energy side of the peak, due to the presence of a small amount of W(V) on the surface. The coloration processes contribute to increase the component at low BE, as confirmed in all

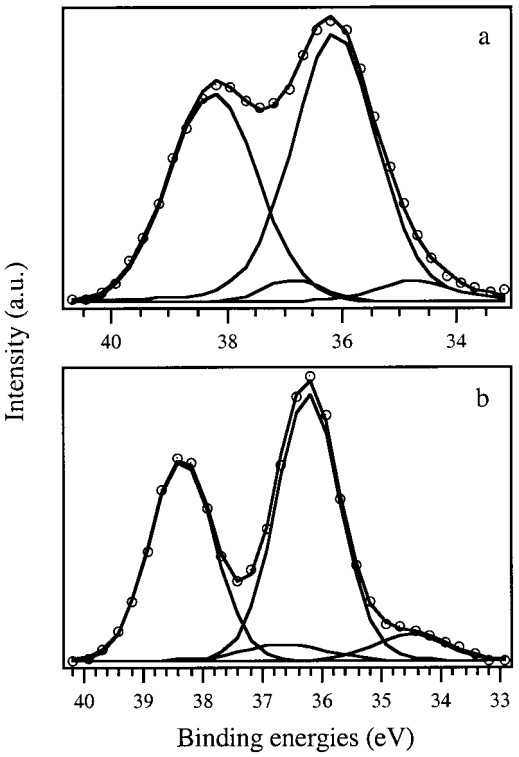

Figure 10. $W4f_{7/2}$ photoelectronic peak of sample 6A before (a) and after (b) electrochromic coloration.

samples and frequently demonstrated in the literature.[25] In the case of sample 6 the situation is certainly more complex (Figure 10): the W4d double peak is initially broadened, positioned at higher binding energies (due to the high ionicity of this matrix), and characterized by little contribute due to W(V) species, and after coloration it appears modified due to the phenomenon of sharpening of the principal peaks. The chemical environment is quite more defined, a particular phosphorated compound is generated, and the presence of W(V) states is now more evident.

Conclusions

The synthesis of electrochromic films represents an important research area in the material science field. Amorphous tungsten oxide layers are certainly the most important inorganic products and therefore they are frequently studied. In this work we have examined the synthesis of films doped with phosphorus in order to preserve the amorphous condition even after thermal treatment (during or after deposition) at temperatures over the crystallization point of the WO_3 matrix. The synthesis is performed by chemical vapor deposition and the chosen precursors contain the dopant in the first coordination sphere of the metal. The phosphorus content can be modulated mainly by choosing an appropriate precursor; the synthetic conditions (namely, the oxygen partial pressure) are generally not critical. Although the type of doping is uniquely determined, the nature of the phosphate groups present in the matrix is different from case to case, as suggested by FT-IR measurements. This aspect emphasizes the importance

(25) Jeong, J. I.; Hong, J. H.; Moon, J. H.; Kang, J.-S.; Fukuda, Y. *J. Appl. Phys.* **1996**, *79*, 9343.

of a careful choice of the molecular precursor for the synthesis of thin films with the projected properties.

The amount of dopant sufficient to inhibit the crystallization of the growing matrix of tungsten oxide results to be really low (2−4% with respect to the metal) on silicon and a little more (about 10%) on KGlass, a polycrystalline matrix. The isomers **4** and **5** that accomplish this condition are easy to synthesize and to handle; they have low melting points and can be used in a mixture without expensive separation procedures. These aspects suggest an interesting possible application of these precursors in CVD processes for the synthesis of electrochromic devices based on amorphous tungsten oxide.

Higher phosphorus content prevents the films from crystallization processes even after postdeposition thermal treatments; this condition is easily obtained with complexes such as **2**, **3**, or **6**, but in this case the films obtained are more properly defined as phosphotungstic glasses.

From an electrochromical point of view, the results certify that the presence of the dopant, even at low concentration, limits the electrochromic behavior of the samples; in particular, although the electrochromic efficiency of the films appears in some cases to be increased, the absorbance is generally lower with respect to the reference film obtained from $W(CO)_6$. It should be underlined that the reversibility of the system is demonstrated and an improvement of the electrochromic characteristics might be reached by a proper choice of the experimental conditions. An interesting aspect is connected with the behavior of the P-rich layer obtained from complex 6. Electrochromic analysis demonstrates that this material is different from those obtained with the other precursors. In particular, the appearance of a different electrochromic mechanism at high negative potentials is quite surprising. This is probably due to an electrochemical or electrochemically induced structural modification of the material. More precisely, even if in this work the presence of W(IV) sites on the film surface was not ascertained, we think that the appearance of this oxidation state (by reduction of the W(V) or reorganization of the oxygen coordination sphere around the metallic center) could justify the particular nature and the absorption wavelength in these films.

Some interesting features of our approach to amorphous WO_3 thin layers should be underlined. The use of molecular tungsten precursors containing the P dopant is unprecedented (not only for the CVD technique); furthermore, the volatility and thermal stability allow the complex to reach intact the surface of the substrate, favoring a uniform distribution of the W and P centers not only on the surface but also in the bulk. Their atomic ratio can be tuned by a proper choice of the phosphorus ligand. In fact, complexes with similar coordination spheres give different deposition products. For example, substitution of a methyl in precursor **2** with an ethyl group (**3**) produces quite different FT-IR patterns of the films; more remarkably, the $P(OEt)_3$ groups of **6** decompose, on the growing matrix, very differently from PEt_3, as a consequence of specific ligand to matrix interactions. This last point emphasizes the potentiality of these synthetic procedures, which can be easily extended to organometallic precursors containing ligands with properly designed grafting groups and with dopant atoms different from phosphorus.

Acknowledgment. The authors thank Mr. A. Ravazzolo for his technical support and skill and Dr. P. Pastore for his suggestions in the development of the apparatus for electrochemical measurements. Moreover, particular thanks to all young researchers of the XPS laboratory for their important technical support and suggestions. This work was supported by the CNR (Consiglio Nazionale delle Ricerche) and by MURST (Ministero per l'Università e la Ricerca Scientifica e Tecnologica).

CM980741N